Int. J. Heat Mass Transfer. Vol. 34, No. 11, pp. 2921–2924, 1991
Printed in Great Britain

0017–9310/91 $3.00 + 0.00

TECHNICAL NOTES

Non-Fourier effect on heat conduction during welding

H. Q. YANG
CFD Research Corp., 3325-D Triana Blvd., Huntsville, AL 35805, U.S.A.

(*Received* 21 *May* 1990 *and in final form* 22 *January* 1991)

INTRODUCTION

THE KNOWLEDGE of heat transfer during welding is essential to the quality and productivity of the welding products. It is well known that the heat flow experienced by a weldment can significantly influence the pool shape, temperature gradient and cooling rate. On the other hand, the pool shape of the weldment determines the macro-structure of joint, and thermal stresses and the consequent residual stresses are the result of the non-uniform distribution of temperature (non-zero temperature gradient). The thermal history of the weldment is also very important in determining microstructural changes the material undergoes and the strength of the weld joint. It is, therefore, not surprising to notice that a large amount of effort has been devoted to the simulation of detailed temperature distribution during the welding process. Even though various aspects of heat transfer during welding have been thoroughly studied, the effect of non-Fourier conduction, which is due to the consideration of the finite propagation speed of the thermal wave, is not completely understood.

The classical theory of heat conduction, which has been widely adapted in the previous simulation of heat transfer problems during welding, postulates a heat flux to be directly proportional to the temperature gradient in the form

$$q = -k\nabla T. \tag{1}$$

This heat flux responds to temperature variations simultaneously. As a result, any temperature disturbance will propagate at an infinite speed. This physically unacceptable notion of instantaneous energy diffusion will not give reliable results in a short duration of initial transient, or in the situation when thermal travelling speed is not high, such as in the low temperature case. Vernotte [1] suggested a modified flux law of the form

$$\tau\partial q/\partial t + q = -k\nabla T \tag{2}$$

where q is the heat flux, T the temperature, and τ represents a relaxation or start-up time for the commencement of heat flux after a temperature gradient has been imposed on the medium. It is related to the speed of propagation of the thermal wave (c) and thermal diffusivity (α)

$$\tau = \alpha/c^2. \tag{3}$$

Since this model was introduced, the wave nature of heat propagation has been the topic of many investigations [2–4]. In most studies related to hyperbolic heat conduction, the subject of interest was the transient instance during which the thermal wave has not yet travelled through the entire domain. Actually, a hyperbolic length scale, defined as the product of the speed of the thermal wave and the characteristic time, may well indicate the importance of the non-Fourier effect. When the hyperbolic length scale is larger than the physical characteristic length scale, the non-Fourier effect can be neglected and vice versa. In the situation of a moving heat source, such as during welding, the physical characteristic length is the product of the moving speed of the heat source and the characteristic time. Here, the non-Fourier effect prevails not only in the initial transient but also in the entire time duration. One may well appreciate the importance of the non-Fourier effect when the speed of a moving heat source is comparable with the speed of the thermal wave. Indeed once the speed of the heat source is equal to or greater than the speed of the thermal wave, the original elliptic heat conduction equation will become hyperbolic, and a situation may arise which gives discontinuity in temperature and heat flux. This is very similar to the behavior of the Prandtl–Glauert equation describing compressible flow solved by a potential function.

THEORETICAL EQUATIONS AND NUMERICAL SOLUTION

The governing partial differential equation for either a moving point or a line heat source seems to have been first derived by Wilson [5]. Rosenthal [6] independently applied this formulation to the arc weld problem. These references are often quoted and have served as the starting formulation for the papers that followed. It is generally realized that for certain applications not involving complicated weldment geometries, these solutions indeed provide a good prediction of the arc welding process. With the assumption of constant properties and neglected latent heat due to phase change, the equation of energy conservation can be written as

$$\rho c_p(\partial T/\partial t) + \nabla q = 0 \tag{4}$$

where ρ and c_p are material density and specific heat, respectively. Combined with equation (2), it becomes

$$1/c^2\,\partial^2 T/\partial^2 t + 1/\alpha\,\partial T/\partial t = \nabla^2 T. \tag{5}$$

For the welding problem, we are interested in the temperature field observed from a moving system attached to the moving heat source. As shown in Fig. 1, let the fixed Cartesian coordinate system x, y and z be oriented such that the x-axis is along the weld seam and points in the direction of the torch velocity. The z-axis direction is through the plate thickness, while the y-axis is in a direction transverse to the welding direction. Equation (5) describes the three-dimensional heat conduction equation in terms of the fixed coordinate system. The relationship between the fixed coordinates (x, y, z) and moving coordinates (x', y, z) can be expressed in terms of the velocity of the heat source (u)

$$x' = x - ut. \tag{6}$$

This study is concerned with the heat transfer during a quasi-steady state of the welding process in which the welding torch moves with a constant velocity u, and all initial temperature disturbances have died out so that the temperature distribution has reached a steady state with respect to a

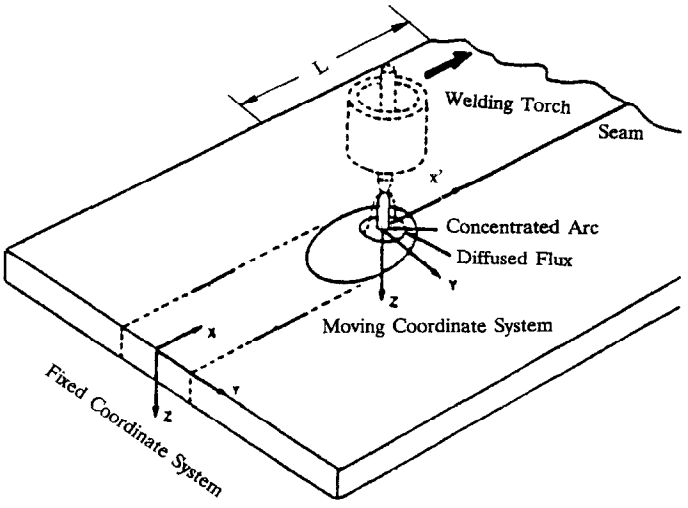

FIG. 1. Schematics of welding process, and reference and moving coordinate systems.

coordinate system moving with the arc (x', y, z). Under this assumption the transient temperature effects can be removed from the formulation. This will make the following transformation possible:

$$\partial T/\partial t = -u\,\partial T/\partial x', \quad \partial^2 T/\partial^2 t = u^2\,\partial^2 T/\partial x'^2,$$
$$\partial^2 T/\partial^2 x = \partial^2 T \partial x'^2. \tag{7}$$

By substituting equation (7) into equation (5), the governing equation valid in the moving coordinate system (x', y, z) is obtained for a quasi-steady state process

$$-u/\alpha\,\partial T/\partial x' = (1-u^2/c^2)\partial^2 T/\partial x'^2 + \partial^2 T/\partial y^2 + \partial^2 T/\partial z^2. \tag{8}$$

Equation (8) is similar to the Euler equation for compressible flow expressed in terms of velocity potential. As in the compressible flow, we define a thermal Mach number M as

$$M = u/c. \tag{9}$$

It is seen that depending on whether M is smaller, equal to, or larger than unity, equation (8) will become elliptic, parabolic or hyperbolic.

A control volume formulation is used in the present study to obtain a numerical solution of the energy equation. The domain of interest is divided into a set of control volumes. A main grid is located at the center of each control volume. The discretization equation for the value of the variable at a grid point is obtained by conserving the flux of this variable over the control volume that surrounds the grid point. For example, by integrating equation (8) over a control volume surrounding the point (i, j, k) we obtain

$$f_{i+1/2,j,k} - f_{i-1/2,j,k} + f_{i,j+1/2,k} - f_{i,j-1/2,k} + f_{i,j,k+1/2} - f_{i,j,k-1/2} = 0 \tag{10}$$

with

$$f_{i+1/2,j,k} = [-u/\alpha\, T_{i+1/2,j,k} - (1-M^2)(\partial T/\partial x)_{i+1/2,j,k}]S_{i+1/2,j,k} \tag{11a}$$

$$f_{i,j+1/2,k} = -(\partial T/\partial y)_{i,j+1/2,k} S_{i,j+1/2,k} \tag{11b}$$

$$f_{i,j,k+1/2} = -(\partial T/\partial z)_{i,j,k+1/2} S_{i,j,k+1/2} \tag{11c}$$

where S is the surface area of the control volume. The diffusive terms are approximated by central difference, while the convective terms are approximated as

$$-u/\alpha\, T_{i+1/2,j,k} = -u/\alpha[(1+\beta)/2 T_{i+1,j,k} + (1-\beta)/2 T_{i,j,k}]. \tag{12}$$

Here β is a damping coefficient. When β is zero, the approximation is equivalent to central difference, while when β is unity, it is upwind difference. With this approximation, one obtains the final discretization equation in the form of

$$A_{i,j,k} T_{i,j,k} = \Sigma A_{NB} T_{NB} \tag{13}$$

with NB denoting the neighboring points, and A as the link coefficient.

To find the solution of equation (8), appropriate boundary conditions must be specified. For temperature they are defined as follows:

$$\text{at } x = L, \quad T = T_0 \tag{14a}$$

$$\text{at } z = 0, \quad -k\,\partial T/\partial z = q(r) \tag{14b}$$

and at other surfaces, an adiabatic condition is used

$$-k\,\partial T/\partial n = 0. \tag{14c}$$

In the above, $q(r)$ is the heat flux supplied by the heat source with a certain distribution. A Gaussian flux distribution for arc heat input has almost invariably been used in the literature, with

$$q(r) = 3Q/(\pi r_b^2)\exp(-3r^2/r_b^2) \tag{15}$$

where Q is the total input, and is assumed to be independent of time. The radius r in equation (15) is the distance from the center of the arc on the surface, and r_b the arc radius describing a region in which 95% of the total heat is deposited on the plate.

Due to symmetry with respect to the weld centerline, the temperature field is calculated only on one side of the centerline. In order to enhance the accuracy of calculation in the high heat input region and to reduce the cost of analysis, grids of variable spacing are used, i.e. finer spacing near the heat source and a coarser grid away from it.

RESULTS AND DISCUSSION

The workpiece considered is 200 mm long (x), 40 mm wide (y) and 6 mm thick (z). The physical properties of k, c_p and ρ are as follows:

$$k = 66\ \text{W m}^{-1}\ \text{K}^{-1}, \quad c_p = 502\ \text{J kg}^{-1}\ \text{K}^{-1}$$
$$\rho = 7870\ \text{kg m}^{-3}. \tag{16}$$

The total heat input is 2128 W. The arc is moving with a speed of 2 mm s^{-1} and the arc beam radius is, as usual, 5 mm. In the numerical model, a non-uniform grid of $90 \times 30 \times 15$ is used.

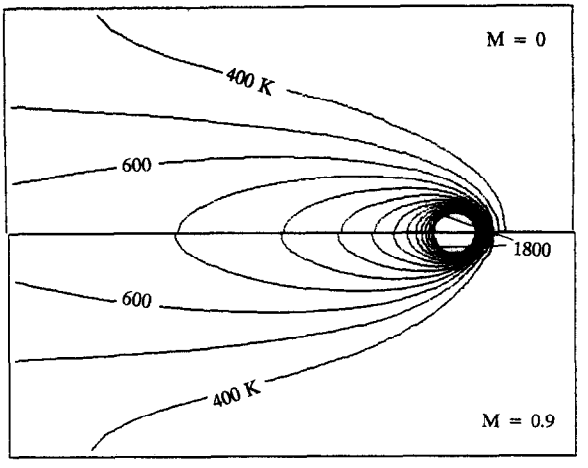

(a) at the top surface

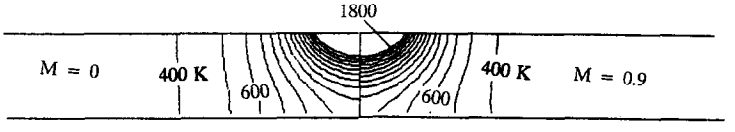

(b) at the transverse plane of $x'=0$

FIG. 2. Temperature contours under condition of $r_b = 5$ mm with $M = 0$ and 0.9 at: (a) the top surface; (b) the transverse plane of $x' = 0$.

Before a meaningful calculation can be made, it is critical to assess the value of thermal wave speed which is related to the relaxation time τ. According to Sieniutycz [7], τ is between 10^{-8} and 10^{-10} s for gases and between 10^{-10} and 10^{-12} s for the liquids and solids. Based on the thermodynamics of irreversible processes, Luikov [8] deduced that for solid aluminum $\tau = 10^{-11}$ s, whereas for capillary-porous bodies, the relaxation time is as much as 10^5–10^7 times higher than that of solid metals. Based on the physical properties given in equation (16), we have

$$c = (\alpha/\tau)^{1/2} = 4.08 \times 10^{-3} \tau^{-1/2} \ (\mathrm{m\ s^{-1}}). \tag{17}$$

For τ within 10^{-10}–10^{-12} it leads to

$$4.08 \times 10^2 \ \mathrm{m\ s^{-1}} < c < 4.08 \times 10^3 \ \mathrm{m\ s^{-1}}. \tag{18}$$

For most welding systems, the speed of the heat source is of the order of 10^{-2} m s^{-1}. As a result, the thermal Mach number is of the order of 10^{-5}–10^{-4}. For such a small thermal Mach number, the non-Fourier effect can be neglected in the analysis for the welding problems.

In the following, attention will be drawn to the hypothetical mathematical exercise which reveals qualitatively the effect of a thermal Mach number if it is large, which may well be realized for the capillary-porous bodies.

Figure 2(a) shows the comparison of temperature contours with thermal Mach numbers of $M = 0$ and 0.9 at the top surface ($z = 0.01$ mm). The level of the temperature contours is from 400 to 1800 K, which is about the melting point of steel. Therefore, the isotherm of 1800 K simply describes the size of the pool shape. In general, there is no significant change visible except in front of the heat source. It is seen that the pre-heating time becomes relatively short due to the non-Fourier effect. From a mathematical point of view, the effect of non-Fourier conduction, with the condition of fixed speed of moving source, is mainly in introducing a non-homogeneous thermal conductivity. The equivalent thermal conductivity is the same as the original one in the y- and z-directions, but is reduced by a factor of $(1-M^2)$ in the x-direction. Due to this lower thermal conductivity in the direction of moving heat source, the temperature gradient in front of the heat source tends to steepen. To gain a general three-dimensional perspective view of the non-Fourier effect, the isotherms in the transverse planes of $x' = 0$ mm, which is the location of the heat source, is shown in Fig. 2(b). Apparently, in the transverse plane along the depth direction there is almost no variation visible, and the heat penetration is also the same.

The temperature profiles along the longitudinal direction (x') at the top surface of $z = 0.01$ mm with $y = 2.5$ mm are plotted in Fig. 3. The thermal Mach numbers here are 0, 0.6, and 0.9. To evaluate the cooling condition the metal undergoes from Fig. 3, the coordinate transformation of equation (6) can be used, where

$$T(x', y, z) = T(x - ut, y, z) \tag{19}$$

and

$$\partial T/\partial t = -u \, \partial T/\partial x'. \tag{20}$$

Indeed, the temperature profile for $x' < 0$ gives a good indication of the cooling rate and the cooling time. Actually, according to equation (19), Fig. 3 can be viewed as the temperature history of a point which has the same coordinate of y and z. As seen from Fig. 3, non-Fourier effects tend to increase the maximum temperature and to give a higher cooling rate. The impact, however, is very minor.

One of the reasons for the phenomena observed above may well be the result of a relatively large heat beam radius (r_b). Therefore, the calculations are further extended to a

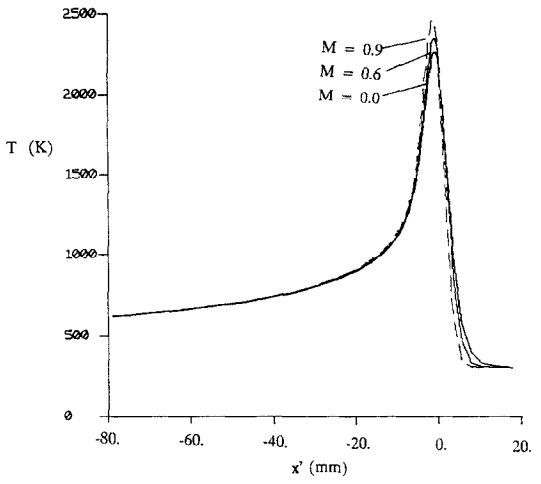

FIG. 3. Temperature profiles under condition of $r_b = 5$ mm along the x-direction at $y = 2.5$ mm.

smaller heat beam radius of $r_b = 0.1$ mm. This corresponds to laser or electron beam welding. Here the rest of the physical parameters remain the same. As seen from Fig. 4(a), the pre-heat time is now dramatically reduced with a sharp heat front on the top surface. The pool shape reduces in the x-direction but enlarges in the y- and z-directions (Fig. 4(b)). Away from the heat source, no significant change is found.

In conclusion, the effect of the non-Fourier conduction on welding heat conduction is to reduce the equivalent heat conductivity in the direction of a moving heat source. This effect is negligibly small because of the high speed of the thermal wave. The hypothetical exercise indicates that at a relatively large r_b, the non-Fourier effect tends to reduce the pre-heating time while the changes in the others are minor. At a smaller r_b, it tends to increase the maximum temperature and cooling rate in the heat-affected zone, and to deform the pool shape.

REFERENCES

1. M. P. Vernotte, Les paradoxes de la theorie continue de l'equation de la cgaleur, *Comp. Rendus* **246,** 3145–3155 (1958).
2. D. C. Wiggert, Analysis of early-time transient heat conduction by method of characteristics, *ASME J. Heat Transfer* **99,** 35–40 (1977).
3. D. E. Glass, M. N. Ozisik, D. S. McRae and B. Vick, On the numerical solution of hyperbolic heat conduction, *Numer. Heat Transfer* **8,** 497–504 (1985).
4. H. Q. Yang, Characteristic-based, high-order non-oscillatory numerical method for hyperbolic heat conduction, *Numer. Heat Transfer*, Part B **18,** 221–241 (1990).
5. H. A. Wilson, On heat convection, *Proc. Camb. Phil. Soc.* **12,** 406–423 (1904).
6. D. Rosenthal, The theory of moving source of heat and its application to metal treatments, *Trans. ASME* **68,** 849–866 (1946).
7. S. Sieniutycz, The variational principle of classical type for non-coupled non-stationary irreversible transport processes with convective motion and relaxation, *Int. J. Heat Mass Transfer* **20,** 1221–1231 (1977).
8. A. V. Luikov, Application of irreversible thermodynamic method to investigation of heat and mass transfer, *Int. J. Heat Mass Transfer* **9,** 139–152 (1966).

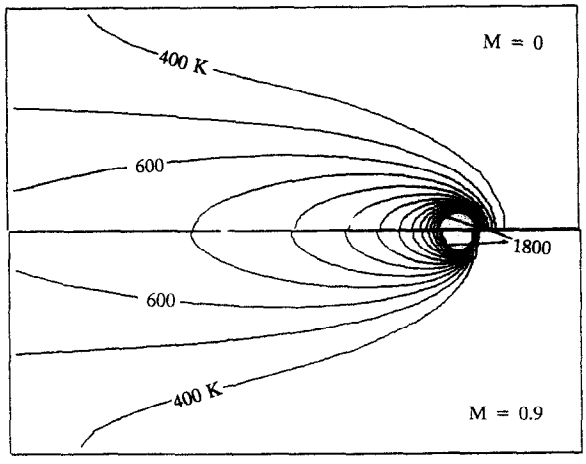

(a) at the top surface

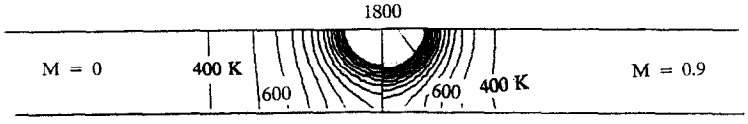

(b) at the transverse plane of x'=0

FIG. 4. Temperature contours under condition of $r_b = 0.1$ mm with $M = 0$ and 0.9 at: (a) the top surface; (b) the transverse plane of $x' = 0$.